PHYSICAL REVIEW B VOLUME 2, NUMBER 7 1 OCTOBER 1970

Nuclear Relaxation in Ferromagnetic Cobalt

Earl David Shaw*
Department of Physics, University of California, and Inorganic Materials Research Division, Lawrence Radiation Laboratory, Berkeley, California 94720
(Received 27 February 1970)

Nuclear-magnetic spin-spin relaxation processes of Co^{59} have been studied in magnetically saturated particles of fcc cobalt. The transverse relaxation has been studied experimentally by observing the two-rf-pulse spin-echo envelope decay. This decay is initially oscillatory, with the oscillations damping in a time of order of the transverse-relaxation time T_2 into exponential decay. The oscillatory behavior is dependent on the pulse widths, and the relaxation time T_2, determined from the exponential decay rate, varies as the square root of the local field. Theory is presented which shows that the observed oscillatory behavior can be explained qualitatively by assuming that the dominant spin-spin interaction is of the Suhl-Nakamura type, with the resonance line broadened by microscopic inhomogeneities. The period of the oscillations gives the rms microscopic inhomogeneous linewidth 100 kHz. Using the correlation-function technique, the relaxation function has been derived for this system. This theory is similar to that of Kubo and Tomita for the exchange-narrowing problem, and agrees well with the observed nonoscillatory transverse relaxation. From the derived relaxation function and observed transverse-relaxation results, a model of the homogeneous line is deduced. The line is assumed to be Lorentzian, with a cutoff of the order of the second moment of the Suhl-Nakamura interaction. Using this model and the theory of quantum statistics of irreversible processes, a theory of spectral diffusion is derived. Spectral diffusion was studied experimentally by monitoring the decay of the three-rf-pulse–stimulated echo. The new theory presented here agrees well with these experimental results.

I. INTRODUCTION

Since the discovery of the Co^{59} resonance in ferromagnetic cobalt, [1] a considerable amount of work has been performed on this system. And yet, even though from the beginning it was believed that the dominant spin-spin mechanism in moderate dc magnetic fields was the Suhl-Nakamura interaction[2] (indirect virtual spin-wave coupling) weakened by random microscopic static inhomogeneities, it was not until a preliminary account of this study[3] that direct experimental evidence was reported which supported that conclusion. The purpose of this paper is to describe quantitatively the spin-spin processes in magnetically saturated particles of cobalt, in applied dc magnetic fields where the weakened Suhl-Nakamura interaction is the dominant nuclear-coupling mechanism.

In order to study the microscopic spin-spin processes in ferromagnetic cobalt, a two-rf-pulse spin-echo study was made on magnetically saturated particles. The measurements were made in dc applied fields of moderate magnitude and will be described in Sec. II. Along with the experimental results, new theoretical results are presented in this section to interpret the experimental observations. An echo amplitude oscillatory effect observed experimentally is shown to be caused by pair coherence between nearest-neighbor spins, in different local fields, coupled by the Suhl-Nakamura interaction. The period of the oscillations gives a measure of the rms microscopic inhomogeneous linewidth analogous to the earlier results of Hahn and Maxwell for exchange-coupled systems. [4] Using the correlation-function technique, a theory is derived similar to that of Kubo and Tomita for exchange narrowing, [5] that describes accurately the observed nonoscillatory relaxation process. In particular, the decay law is shown to be initially Gaussian, proceeding to exponential decay at long times. This prediction is in agreement with the experimental results. Also, the derived analytic expression for the relaxation rate at long times has the observed dependence on the local dc magnetic field. The change of decay law with time is shown to be a result of the more stringent requirement on energy conservation for mutual spin flips at long times. This is a special application of the uncertainty principle. Thus, the correlation-function approach gives results which extend earlier theoretical results of Portis[6] and of Hone, Jaccarino, Ngwe, and Pincus. [7] Analogous to the Anderson model for exchange narrowing, [8] a model of the homogeneous line is deduced in this section. The spectral distribution of the homogeneous line is taken to be Lorentzian with a cutoff of the order of the second moment of the Suhl-Nakamura interaction. The experimental data are used to make the choice of cutoff more precise.

Portis[6] pointed out previously that macroscopic spectral diffusion is possible in a system where the inhomogeneity varies microscopically. These con-

siderations are made more quantitative in Sec. III. For the case where the transverse-relaxation time is much shorter than the longitudinal-relaxation time, a theory of spectral diffusion is derived using the model of the homogeneous line deduced in Sec. II and recent developments in the formulation of the theory of quantum statistics of irreversible processes.[9-11] These results are compared with the experimental results of the three-pulse-stimulated echo study presented in this section.[12] It is thus demonstrated that the microscopic and macroscopic spin-spin processes can be treated in a unified manner in this system.

II. TRANSVERSE RELAXATION

A. Experimental Results

The familiar two-pulse spin-echo technique[13] was used to study a cobalt metal sample consisting of Johnson-Matthey cobalt sponge. These μ-sized particles, which are fcc and multidomain in zero dc field, were studied at 77 °K in dc applied magnetic fields between 5 and 10 kOe. Multidomain particles become magnetically saturated in dc fields in excess of the particle demagnetizing fields. However, for the range of applied fields utilized in this study, not all of the particles in the sample were saturated. Since there is a distribution of particle shapes and a random orientation of the particles with respect to the dc magnetic field, the sample has a distribution of particles with demagnetizing factors varying between 0 and 4π. Thus, fields in excess of $4\pi M = 18$ kOe are required to saturate the *entire* sample. However, at these fields, the dipole spin-spin interaction becomes comparable to the Suhl-Nakamura interaction,[14]

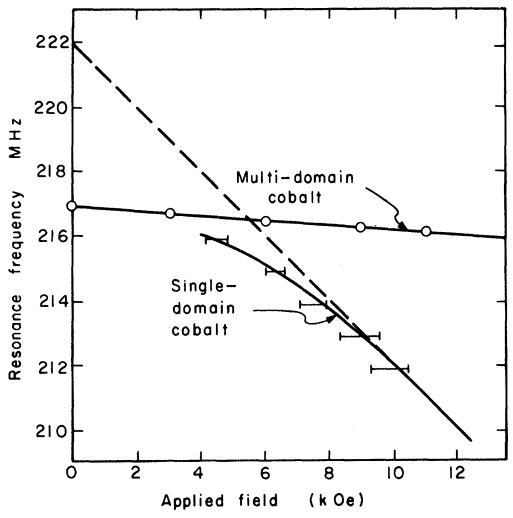

FIG. 1. Resonance frequency of Co^{59} as a function of applied field in cobalt sponge.

and it is the aim here to study the latter interaction under as unambiguous conditions as possible. In order to separate the signal of single-domain particles from that of multidomain particles, advantage was taken of the different field dependence of the ferromagnetic-nuclear-resonant (FNR) frequency for the two cases.[15] If the turning angle of the pulses is small, as is the case in this study, it is possible to distinguish two signals. One has large amplitude at low dc fields, strong amplitude dependence on field, and very weak frequency dependence on field as illustrated in Fig. 1. This signal characterizes the multidomain material. The second signal is extremely broad and of considerably smaller amplitude at low fields; the amplitude varies less strongly with field; and the resonant frequency varies much more strongly, approaching a linear dependence on the applied field at large fields as seen in Fig. 1. This signal characterizes the single-domain material.[15] The resonant frequency decreases with increasing field because the hyperfine field at the cobalt nucleus is negative. The broadness of the single-domain signal is associated with the distribution of demagnetizing factors. The width of the line is approximately 18 MHz, corresponding to the local-field spread of 18 kOe. All measurements were made on the single-domain signal at small-pulse turning angles.

The rf field was applied perpendicular to the dc magnetic field in order to take advantage of the added enhancement of the rf signal by domain rotation. The enhancement factor is estimated to vary between 40 and 20 for dc field values from 5 to 10 kOe, respectively. The half-width of the echo envelope T_2^* varied from 0.75 to 1.5 μsec for these fields. Therefore, the width of the excited spectrum was of the order of $(1/2\pi)(2/T_2^*) \cong 400-200$ kHz. Thus, a narrow portion of the single-domain spectrum was sampled at each field value.

The first pulse of the two-pulse spin-echo sequence was adjusted for maximum signal, and this pulse will be *assumed* to be a 90° pulse. The results of monitoring the spin-echo amplitude for $90°-\beta$ pulse sequences at fixed frequency 215.9 MHz for values of $\beta = 90°$, 135°, and 180°, are shown in Fig. 2. The time τ is the separation between the first and second pulse, and the second pulse and the center of the echo. For $\beta = 180°$, the time behavior at moderately short times is essentially a Gaussian decay transforming into exponential decay at long times. The exponential-decay behavior was observed out to 100 μsec. For τ less than about 2 μsec ($2\tau \lesssim 4$ μsec) receiver saturation due to the large pulses and interference between the spin-echo and free-induction decay signal[13] obscures the dependence of the echo amplitude

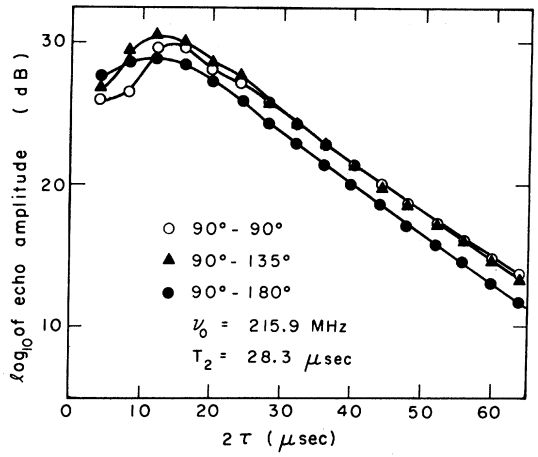

FIG. 2. Log_{10} of the spin-echo amplitude versus time for several turning angles.

time behavior on the homogeneous broadening processes.[16] These effects may contribute to the decrease of the $\beta = 180°$ curve at $2\tau = 4$ μsec. For $\beta \neq 180°$, there is a much more noticeable spin-echo amplitude oscillatory effect superimposed on the $\beta = 180°$ curve at short times. The period of these oscillations in τ is approximately 7 μsec $\pm 10\%$. This corresponds to a frequency of 140 kHz $\pm 10\%$. These oscillations damp out in a time of order of the spin-spin relaxation time $T_2 = 28.3$ μsec determined from the slope of the exponential curve. T_2 does not depend on β within the experimental accuracy of 10%.

The frequency dependence of the echo decay is shown in Fig. 3 for a 90°-90° pulse sequence. The oscillatory behavior is less apparent at lower

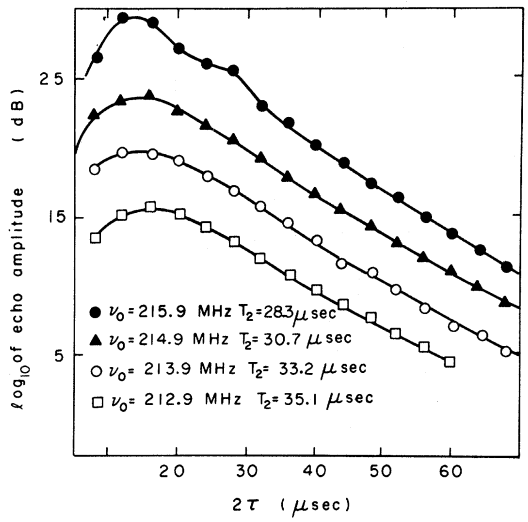

FIG. 3. Log_{10} of the echo amplitude versus time and frequency for a 90°-90° pulse sequence.

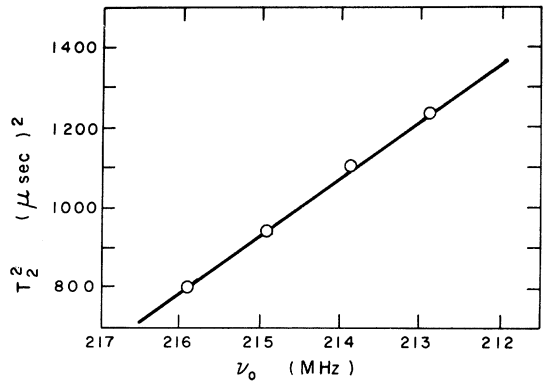

FIG. 4. The square of transverse-relaxation time versus frequency.

frequencies where the enhancement factor is smaller and thus the signal is smaller. The interpretation of the results at $2\tau = 8$ μsec is also made more difficult by the increase in T_2^* at lower frequencies because of the decrease in enhancement factor. The relaxation time T_2 monotonically increases with decreasing frequency. The increase in T_2 indicates that the spin-spin coupling is weakened by the increase of the local field. In Fig. 4, T_2^2 is plotted versus the resonance frequency.[3] The data are fit well by a straight line that extrapolates to a frequency of 221.5 MHz for $T_2^2 = 0$. This is 4.6 MHz above the zero-field multidomain resonance. In this paper these results are shown to be direct evidence that the Suhl-Nakamura interaction, weakened by microscopic inhomogeneities, is the dominant homogeneous broadening mechanism for the range of applied dc fields of 5–10 kOe.

B. Microscopic Theory

1. *Hamiltonian of System*

The Hamiltonian $\mathcal{H}$ of the N-particle system consists of two terms: the Zeeman energy $\mathcal{H}_Z$, and the spin-spin interaction term $\mathcal{H}_{SN}$[17];

$$\mathcal{H} = \mathcal{H}_Z + \mathcal{H}_{SN} = -\hbar \sum_l \omega_l I_l^z + \sum_{l \neq m} \sum_m A_{lm} I_l^+ I_m^- \,, \tag{1}$$

$$A_{lm} = \frac{-\hbar^2 \omega_0^2}{2SN} \sum_{\vec{k}} \frac{e^{-i\vec{k}\cdot\vec{r}_{lm}}}{E_{\vec{k}}} \,.$$

S is the effective electronic spin; $\vec{k}$ is the spin-wave wave number; $E_{\vec{k}}$ is the unperturbed (by nuclear effects) spin-wave energy for the wave number $\vec{k}$; ω_0 is taken to be the center frequency of the resonant spins; ω_l is the frequency of the nuclear spin located at the lth site; $\vec{r}_{lm}$ is the vector between the lth and mth sites; and $I_l^{z,+,-}$ are the nuclear angular momentum operators having the usual meaning. Although A_{lm} is frequency dependent, it

does not vary appreciably for the width of the spectrum excited experimentally, or for the range of frequencies (approximately $1/T_2$) over which spins of different frequency interact. The N spins are assumed to be within the microscopic range of the Suhl-Nakamura interaction, and their frequencies are assumed to be randomly distributed about ω_0 with the spread described by the normalized distribution function $g(\omega-\omega_0)$. $E_{\vec{k}}$ is derived in Ref. 18 for an isolated single-domain particle and may be written

$$E_{\vec{k}}=\hbar\,(\gamma_e H'_{1oc}+\gamma_e H_a+\omega_E\hat{a}^2\vec{k}^2)^{1/2}(\gamma_e H'_{1oc}+\gamma_e H_a+\omega_E\hat{a}^2\vec{k}^2+\omega_M\sin^2\theta_{\vec{k}})^{1/2}\ ,$$

$$H'_{1oc}=H_0-N^zM,\quad \cos\theta_{\vec{k}}=k_z/|\vec{k}|\ ,$$

$$\omega_M=4\pi\gamma_e M\ .$$

γ_e is the electronic magnetogyric value; N^z is the particle demagnetizing factor; ω_E is the electronic exchange frequency; $\hat{a}^3$ is the volume of a primitive unit cell; and H_a is the anisotropy field assumed directed along the applied field H_0. For cobalt, $H_a=1$ kOe. For a particle immersed in a permeable medium, there are additional contributions to H'_{1oc} from the cavity in which the particle sits and from the outer surface of the sample. This total local field H_{1oc} is also the additional field that nuclei in single-domain particles experience compared to nuclei in multidomain particles.[15] Thus, the shift in frequency ω_{1oc} of the single-domain FNR signal compared to the zero-field multidomain FNR frequency 216.9 MHz is a measure of H_{1oc}. Also, $\omega_{1oc}=\gamma H_{1oc}$, where $\gamma=2\pi\times1.011$ MHz/kOe is the magnetogyric value for Co^{59}. Since the distribution of particle demagnetizing factors is not known, H_{1oc} rather than H_0 is the relevant parameter for analyzing the data.

For $\theta_{\vec{k}}=0$, $E_{\vec{k}}=\hbar(\gamma_e H_{1oc}+\gamma_e H_a+\omega_E\hat{a}^2k^2)$; this leads to the familiar result

$$A_{lm}=\frac{-\hbar\omega_0^2}{8\pi S\omega_E}\,\frac{\hat{a}}{r_{lm}}\exp\left[-\left(\frac{\gamma_E(H_{1oc}+H_a)}{\omega_E}\right)^{1/2}\frac{r_{lm}}{\hat{a}}\right]\ .$$

For $\gamma_e(H_{1oc}+H_a)/\omega_E\approx10^{-3}\ll1$, this result is valid for all values of r_{lm}.[7] The quantity $[\omega_E/\gamma_e(H_{1oc}+H_a)]^{1/2}\hat{a}$, approximately equal to $30\hat{a}$ in cobalt, is the range of the Suhl-Nakamura interaction. However, it can be seen from the functional dependence of $E_{\vec{k}}$ on $\theta_{\vec{k}}$ that the $\theta_{\vec{k}}=0$ approximation does not account for the dipole contribution to the spin-wave energy. This contribution is important for values of $H_{1oc}+H_a$ of the same order as the average value of $\frac{1}{2}4\pi M\sin^2\theta_{\vec{k}}$. For an approximation that takes account of the dipole energy, $E_{\vec{k}}$ is rewritten

$$E_{\vec{k}}\cong\hbar[\gamma_e(H_{1oc}+H_a)+(\omega_M/2)\sin^2\theta_{\vec{k}}+\omega_E\hat{a}^2k^2]\ , \quad (2)$$

for

$$(H_{1oc}+H_a)\approx(\omega_M/2\gamma_e)\langle\sin^2\theta_{\vec{k}}\rangle_{av}=(4\pi/3M)\ .$$

The average value $\langle\sin^2\theta_{\vec{k}}\rangle_{av}=\frac{2}{3}$ is substituted for $\sin^2\theta_{\vec{k}}$ in $E_{\vec{k}}$ to obtain A_{lm} and the second moment of the Suhl-Nakamura interaction ω_{SN}:

$$A_{lm}=-\frac{\hbar\omega_0^2}{8\pi S\omega_E}\,\frac{\hat{a}}{r_{lm}}\times\exp\left[-\left(\frac{\gamma_E(H_{1oc}+H_a+\frac{4}{3}\pi M)}{\omega_E}\right)^{1/2}\frac{r_{lm}}{\hat{a}}\right], \quad (3)$$

$$\omega_{SN}^2=\frac{4}{3}(I)(I+1)\sum_{m\neq l}\frac{A_{lm}^2}{\hbar^2}=\left(\frac{(I)(I+1)}{24\pi S^2}\right)\times\omega_0^2\left(\frac{\omega_0}{\omega_E}\right)^2\left(\frac{\omega_E}{\gamma_E(H_{1oc}+H_a+\frac{4}{3}\pi M)}\right)^{1/2}\ .$$

For $S=0.85$, $I=\frac{7}{2}$, $\omega_0=1.36\times10^9$; $\omega_E/\gamma_E(H_{1oc}+H_a+\frac{4}{3}\pi M)\cong10^3$, $\omega_E=3.9\times10^{13}$/sec; the calculated value of $(\omega_{SN})^{-1}$ is 7 μsec. In this study, $H_{1oc}+H_a\cong2$–6 kOe and $\frac{4}{3}\pi M=6$ kOe. Thus, the neglect of higher-order dipolar effects will produce an estimated error of 35% or less. The average of $(E_{\vec{k}})^{-1}$ over $\theta_{\vec{k}}$, as opposed to the average of $E_{\vec{k}}$ as was presented here, does not significantly change these results.[16] It is clear that the average over $\theta_{\vec{k}}$ which leads to a spherically symmetric interaction is not a true representation of the Suhl-Nakamura interaction. The interaction actually has a longer range in the z direction than in the transverse plane. However, the description of the interaction presented here is adequate to describe the results of this study.

2. *Modulation of Spin-Echo Amplitude*

In order to describe the dynamics of the spin-echo oscillatory effect, the contribution to the echo from a nearest-neighbor pair for a $\frac{1}{2}\pi-\beta$ pulse sequence is calculated. The nearest-neighbor Hamiltonian

$$H_{12}=-\hbar\omega_1I_1^z-\hbar\omega_2I_2^z+A_{12}(I_1^+I_2^-+I_1^-I_2^+)$$

is used to derive the equation of motion of the angular momentum operators:

$$\frac{\partial I_1^+}{\partial t}=-i\omega_1I_1^+-\frac{2iA_{12}}{\hbar}I_1^zI_2^+,$$

$$\frac{\partial I_1^-}{\partial t}=i\omega_1I_1^-+\frac{2iA_{12}}{\hbar}I_1^zI_2^-, \quad (4)$$

$$\frac{\partial I_1^z}{\partial t}=-i\frac{A_{12}}{\hbar}(I_1^+I_2^--I_1^-I_2^+),$$

with similar results for I_2. The spins are assumed to be initially aligned along the z axis, and a $\frac{1}{2}\pi$ pulse applied along the x axis rotates the spins to

the negative y axis. Thus,

$$I^z_{1,2}(0)=0,\quad I^y_{1,2}(0)=-I,\quad I^x_{1,2}(0)=0.$$

The magnitude of the nearest-neighbor interaction

$$|A_{12}|/\hbar\cong\omega_0^2/8\pi S\omega_E=(450\ \mu\text{sec})^{-1}$$

or

$$(2|A_{12}|I/\hbar)=(65\ \mu\text{sec})^{-1}$$

is calculated from Eq. (3). For the case of microscopic inhomogeneous broadening,

$$|\omega_1-\omega_2|\gg(2|A_{12}|/\hbar)I.$$

Thus, for the time that the oscillatory behavior is observed,

$$t\ll\left[\frac{2A_{12}I}{\hbar}\left(\frac{4A_{12}I}{\sqrt{2}\hbar|\omega_1-\omega_2|}\right)\right]^{-1}\cong 2\text{ msec},$$

the second term in the equation of motion for the transverse component of angular momentum can be neglected. Then,

$$I_1^+(t)=-iIe^{-i\omega_1 t},\quad I_1^-(t)=iIe^{i\omega_1 t},$$

$$I_2^+(t)=-iIe^{-i\omega_2 t},\quad I_2^-(t)=iIe^{i\omega_2 t}.$$

Substituting these equations into the equation of motion for the z component of angular momentum, the solution at the time of the second pulse is

$$I_1^z(\tau)=\frac{4A_{12}I^2}{\hbar(\omega_2-\omega_1)}\sin^2(\omega_2-\omega_1)\tfrac{1}{2}\tau=-I_2^z(\tau).\qquad(5)$$

This oscillatory behavior of the z component of angular momentum is the origin of the observed modulation of the echo amplitude. If a 90° pulse is applied at τ, this component of magnetization will be rotated into the transverse plane. For the times considered here, the individual transverse angular momentum component simply rotates in the plane at the frequency determined by the static field which each spin experiences. Immediately after the 90° pulse, the contribution to the magnetization in the transverse plane is zero, since the two spins give opposite contributions. However, the spins rotate at different frequencies, and this will add an oscillatory contribution to the echo. This signal gives the observed dependence on pulse width; for example, it gives zero contribution to the echo for $\beta=180°$. The prediction that the Suhl-Nakamura interaction will not give a modulation effect for a 90°–180° pulse sequence is consistent with the earlier results of Stearns.[19] Note that for either $A_{12}=0$, or $\omega_1-\omega_2=0$, or if one spin is not resonated, $I^+(0)=0$, the modulation does not occur. This is analogous to the result of Hahn and Maxwell,[4] for exchange-coupled spin pairs. Hahn[13] has shown that the nonoscillatory echo amplitude is proportional to $\sin^2\frac{1}{2}\beta$.

It is now shown how this echo-amplitude dependence on β is modified by the effect of pair coherence. Consider the reference frame that rotates at the rf-pulse frequency ω_0. Both rf pulses are assumed to occur along the x axis in this frame, then the echo signal occurs along the positive y axis at time 2τ. For $\omega_1>\omega_2$, $A_{12}<0$, $\beta\leq\pi$, the pair coherence contributes

$$(\sin\beta)I_1^z(\tau)[\cos(\omega_2-\omega_0)\tau-\cos(\omega_1-\omega_0)\tau]$$

to the magnetization along the positive y axis at 2τ. Thus, the echo amplitude $E(2\tau)$ may be written

$$E(2\tau)\propto 2I\{\sin^2\tfrac{1}{2}\beta-\sin\beta[4A_{12}I/\hbar(\omega_2-\omega_1)]\times\sin^3(\omega_2-\omega_1)\tfrac{1}{2}\tau\,\sin(\omega_1+\omega_2-2\omega_0)\tfrac{1}{2}\tau\}.$$

Pairs of spins such that $\omega_1+\omega_2=2\omega_0$ do not contribute to the modulation of the echo. Since the oscillatory term is only affected by the magnitude of the frequency difference, the rms of the frequency terms is taken in order to give physical interpretation to the measured modulation period. The rms standard deviation of $g(\omega-\omega_0)$ is represented by σ, and since

$$\langle(\omega_1-\omega_2)^2\rangle=\langle(\omega_1+\omega_2-2\omega_0)^2\rangle=2\sigma^2,$$

the final result is written

$$E(2\tau)\propto 2I\left[\sin^2\tfrac{1}{2}\beta-|\sin\beta|\frac{4|A_{12}|I}{\sqrt{2}\hbar\sigma}\sin^4\tfrac{1}{2}\sqrt{2}\sigma\tau\right].\qquad(6)$$

The period of the oscillations in τ is given by $(\sqrt{2}\sigma/2\pi)^{-1}$. Therefore, the observed results give $\sigma/2\pi\cong 100\,\text{kHz}\pm 10\%$ as a measure of the microscopic-inhomogeneity linewidth. This result is in qualitative agreement with results reported in Ref. 12 where an estimate of 140 kHz was given. The ratio of the oscillation amplitude to the echo amplitude is

$$2(2A_{12}I/\hbar)(1/\sqrt{2}\sigma)\cong-30\text{ dB}.$$

These results are consistent with the observations plotted in Figs. 2 and 3. The pair coherence is expected to be rapidly damped since the Suhl-Nakamura interaction is long range and many spins are in communication. The oscillations should thus damp out in a time of order $T_2\cong 30\ \mu$sec as observed. This justifies the earlier approximations which were based on the coherence being observed for a time short compared to the nearest-neighbor spin-spin relaxation time.

3. *Spin-Spin Relaxation Theory*

The nonoscillatory decay of the spin-echo amplitude describes the homogeneous broadening processes.[13] The decay function is given by the Fourier transform of the homogeneous line and can be calculated from the correlation function

$\langle I_l^+(t) I_l^-(0)\rangle$.[20] The high-temperature approximation is valid for the work considered here and simplifies the calculation considerably. For example, nuclear spin-wave effects, which would cause spatial correlation between nuclear spins located at different sites, have no effect on the results reported here. The terms that would lead to such effects are neglected in the following calculation. The equation of motion of $\langle I_l^+(t) I_l^-(0)\rangle$ is calculated from the equation of motion of $I_l^+(t)$. The latter equations are written

$$\frac{\partial I_l^+}{\partial t} = -i\omega_l I_l^+ - \frac{2i}{\hbar}\sum_{m\neq l} A_{lm} I_l^z I_m^+ ,$$

$$\frac{\partial I_l^z}{\partial t} = -\frac{i}{\hbar}\sum_{m\neq l} A_{lm}(I_l^+ I_m^- - I_l^- I_m^+) .$$

The equation for I_l^z is solved and substituted into the equation for I_l^+ to give

$$\frac{\partial I_l^+(t)}{\partial t} = -i\omega_l I_l^+(t) - \frac{2i}{\hbar}\sum_{m\neq l} A_{lm} I_l^z(0) I_m^+(t) - \frac{2}{\hbar^2}\sum_{j\neq l}\sum_{m\neq l} A_{lm}A_{lj} \times \int_0^t [I_l^+(t') I_m^-(t') - I_l^-(t') I_m^+(t')] I_j^+(t)\, dt' .$$

This equation is multiplied by $I_l^-(0)$ and the ensemble average is taken. The first term on the right-hand side of the equality sign gives a Zeeman energy driving term. In the high-temperature approximation, the second term leads to a product term $\langle I_m^+(t)\rangle\langle I_l^z(0) I_l^-(0)\rangle$, and gives zero contribution since the trace of the angular momentum operator is zero. Likewise, the correlation of the four product terms leads to a product of pair correlation functions,

$$[\langle I_l^+(t') I_l^-(0)\rangle\langle I_j^-(t') I_j^+(t)\rangle - \langle I_l^-(t') I_l^-(0)\rangle\langle I_j^+(t') I_j^+(t)\rangle]\delta_{mj} ,$$

with the negative term, which involves double spin-flip processes, giving zero contribution since the Hamiltonian has no terms that will support such processes. To eliminate the Zeeman driving term, the relaxation function $\phi(t)$ is defined by

$$\langle I_l^+(t) I_l^-(0)\rangle = \langle I_l^+(0) I_l^-(0)\rangle e^{-i\omega_l t}\phi_{\omega_l}(t) .$$

ϕ_{ω_l} has the following general properties[9]:

$$\phi_{\omega_l}(t) = \phi_{\omega_l}(-t), \quad \phi_{\omega_l}(0) = 1 ,$$

and is given directly by the decay of the spin-echo amplitude.[16] Ignoring a frequency-pulling term of order $1/T_2$,[16] and interchanging the operation of differentiation with the ensemble average, the following equation of motion for $\phi_{\omega_l}(t)$ is derived:

$$\frac{\partial\phi_{\omega_l}(t)}{\partial t} = -\frac{4}{3}(I)(I+1)\sum_{j\neq l}\frac{A_{lj}^2}{\hbar^2}\int_0^t \phi_{\omega_l}(t')\phi_{\omega_j}(t'-t) \times \cos[(\omega_j-\omega_l)(t-t')]\, dt' , \tag{7}$$

where

$$\langle I_l^+(0) I_l^-(0)\rangle = \tfrac{2}{3}(I)(I+1) .$$

From the uncertainty principle, energy conservation is not a critical consideration at sufficiently small times. In this limit, let

$$\phi_{\omega_l}(t') = \phi_{\omega_j}(t-t') = 1$$

and $\omega_l = \omega_j$ in Eq. (7), then

$$\phi(t) = 1 - \tfrac{1}{2}\omega_{SN}^2 t^2 \approx e^{-\omega_{SN}^2 t^2/2} \tag{8}$$

for

$$\omega_{SN}^2 = \tfrac{4}{3}(I)(I+1)\sum_{j\neq l}(A_{lj}^2/\hbar^2) .$$

Thus, the relaxation is initially Guassian as it is in a concentrated homogeneous system. This result is consistent with the theoretical findings of Klauder and Anderson who predict "Lorentzian diffusion" in a concentrated homogeneous system,[21] and it agrees with the results of Hone, Jaccarino, Ngwe, and Pincus[7] who predict Gaussian decay for the Suhl-Nakamura interaction, in a concentrated homogeneous system, from moment analysis. Also, Eq. (8) is consistent with the short-time experimental observations plotted in Figs. 2 and 3.

To consider the long-time behavior, it is necessary to assume that the microscopic inhomogeneity is random and use the distribution function $g(\omega_j-\omega_0)$ to average frequency over position in Eq. (7). This procedure was first suggested in Ref. 6 and should be a good approximation since each spin interacts with some $(30)^3$ other neighboring spins. If the average is taken in Eq. (7), then the sum over position can be made, and if τ is substituted for $t-t'$, Eq. (7) becomes

$$\frac{\partial\phi_{\omega_l}}{\partial t} = -\omega_{SN}^2\int_{-\infty}^{\infty}\int_0^t \phi_{\omega_l}(t-\tau)\phi_{\omega_j}(\tau) g(\omega_j-\omega_0) \times \cos(\omega_j-\omega_l)\tau\, d\tau\, d\omega_j . \tag{9}$$

As t approaches ∞, the trigonometric term oscillates rapidly for $\omega_j \neq \omega_l$ giving zero contribution to the integral. Since spins interact only with other spins of the same frequency, the spin system becomes essentially diluted in this limit. In the limit of extreme microscopic-inhomogeneous broadening (extreme dilution), it is reasonable to expect the decay to be exponential; particularly, in the light of our experimental results in Figs. 2 and 3. In this limit, $\phi(t-\tau)\,\phi(\tau) = \phi(t)$, and Eq. (9) becomes

$$\frac{\partial\phi_{\omega_l}}{\partial t} = -\omega_{SN}^2\phi_{\omega_l}(t)\left(\lim_{t\to\infty}\int_{-\infty}^{\infty}\int_0^t g(\omega_j-\omega_0)\right.$$

$$\times \cos(\omega_j - \omega_l)\tau \, d\tau \, d\omega_j \Big)$$

$$= -\pi\omega_{SN}^2 g(\omega_l - \omega_0)\phi_{\omega_l}(t), \quad (10)$$

thus,

$$\phi_{\omega_l}(t) = \exp[-t/T_2(\omega_l)] \ ,$$

where

$$1/T_2(\omega_l) = \pi\omega_{SN}^2 g(\omega_l - \omega_0) .$$

This solution is consistent with the second-order iteration solution of Eq. (9) in the long time limit.[16]

This theory contains the essential features of the observed relaxation measurements; it predicts Gaussian decay at short times and Lorentzian decay at long times. The relaxation time at long times is given by

$$1/T_2(\omega_0) = \pi\omega_{SN}^2 g(0) = (\tfrac{1}{2}\pi)^{1/2}\omega_{SN}^2/\sigma$$

for $g(\omega - \omega_0)$ assumed Gaussian. Taking the observed value for $T_2 = 28.3$ μsec, measured at 215.9 MHz, and the measured value for $\sigma/2\pi = 100$ kHz, $(\omega_{SN})^{-1} = 7.5$ μsec is calculated. This is, within all estimated experimental uncertainty, equal to the value of 7 μsec calculated above. Also, the expression for T_2 predicts the linear dependence of T_2^2 on the local field, giving

$$T_2^2 \propto \omega_{SN}^{-4} \propto H_{loc} + H_a + \tfrac{4}{3}\pi M.$$

The value of ω_{loc}/γ for which $T_2^2 = 0$ gives the value of the quantity $H_a + \frac{4}{3}\pi M$. The predicted value of 5–7 kOe corresponding, respectively, to H_a being antiparallel and parallel to the magnetization is reasonably close to the measured value of 4.6 kOe. Again this agreement is within all estimated uncertainty. Note that the $\theta_{\vec{k}} = 0$ approximation would predict an intercept of $H_a = 1$ kOe which is far in error of the observed results.

C. Conclusions

A quantitative description of the homogeneous line has been made. The homogeneous spectrum distribution is the Fourier transform of the relaxation function and is thus Lorentzian near the center of the line, with the linewidth given by T_2^{-1}, and Gaussian in the wings. The Gaussian behavior occurs for spins at a distance of the order of the second moment of the Suhl-Nakamura interaction from the center of the line. For simplicity, the line is considered to be Lorentzian with a cutoff at $\frac{1}{2}\omega_{SN}$. This value is determined from the data in Figs. 2 and 3, since it is at time $(\frac{1}{2}\omega_{SN})^{-1} = 15$ μsec that the exponential decay becomes a fair approximation of the actual relaxation process. The homogeneous "packet" of spins[22] is essentially independent of other packets since different packets experience different static fields. Since spins interact only with spins in the same packet, spectral diffusion must occur within the homogeneous line. Thus, the relaxation function contains the microscopic physics for the macroscopic diffusion process. This is shown formally in Sec. III where a theory of spectral diffusion is derived and compared with experimental results.

III. SPECTRAL DIFFUSION

A. Experimental Results

Spectral diffusion may be studied by monitoring the three-pulse–stimulated echo.[12] After a pair of 90° pulses separated by a time τ, a spin system will have a periodic variation of the z component of angular momentum proportional to $\langle I^z(\omega)\rangle_L \times \cos(\omega - \omega_0)\tau$. Here $\langle I^z(\omega)\rangle_L$ is the z component of the angular momentum density function

$$\langle I^z(\omega)\rangle_L = \left\langle \sum_{l \in \omega} I_l^z \right\rangle_L \ ,$$

where the summation is over all spins that have frequency ω, and the ensemble average is over the equilibrium density matrix. This modulation will be destroyed by spectral diffusion as well as other longitudinal-relaxation processes. However, since only the spectral-diffusion relaxation rate is dependent on τ, the spectral-diffusion effect can be distinguished from other longitudinal-relaxation processes.[12] Following a third 90° pulse at time T, a spin-echo signal occurs at time $T + \tau$ whose amplitude depends on the remaining periodic variation of the z component of angular momentum.[13] In Fig. 5, the $\log_{10}$ of the stimulated-echo signal at 215.9 MHz is plotted versus T for $\tau = 2, 9$, and 13.8 μsec. The decay is initially nonexponential, proceeding to exponential decay at long times. The rate of decay is τ dependent at both long and short times with

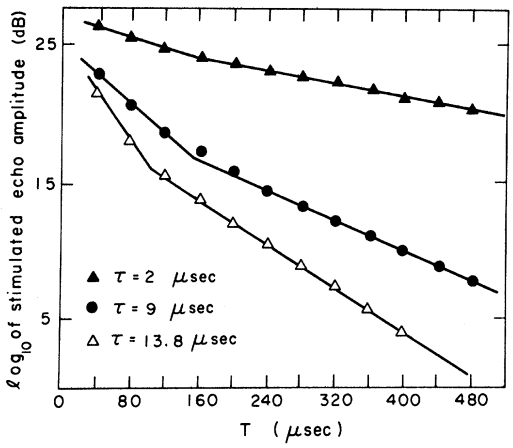

FIG. 5. Log_{10} of the stimulated-echo amplitude versus T and τ.

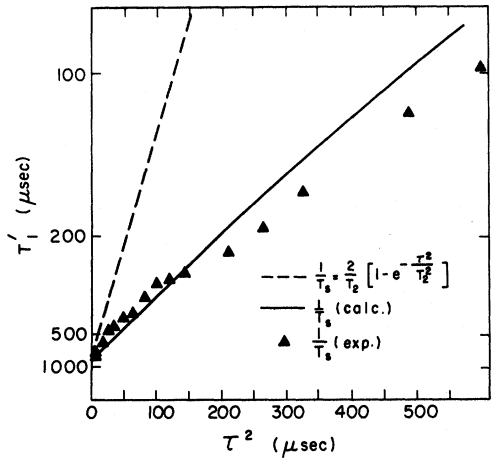

FIG. 6. Longitudinal relaxation rate versus τ^2 at 215.9 MHz.

the rate of decay at short times roughly twice the rate at long times. Because of the τ dependence, the nonexponential behavior is associated with the spectral-diffusion relaxation process.

Within the noise limitation of the experimental apparatus, the slowest relaxation rate was measured from the slope of the exponential curve for several τ values and plotted versus τ^2 in Fig. 6. The overall accuracy is estimated to be within 20%. Initially, the decay rate is proportional to τ^2 as expected from previous results.[12] From the slope of the curve near $\tau^2 = 0$, $D = 3.77 \times 10^{-5} (\mu\text{sec})^{-3} = 0.85/T_2^3$, is determined as a lower limit for the diffusion constant of the system. For large τ, the relaxation rate increases more slowly than τ^2. In Fig. 7, the relaxation rate for several values of the local field is plotted versus τ^2. It is seen that for this range of field values, the diffusion process is essentially independent of field. The slight tendency for the points of the 213.9-MHz curves to give larger relaxation rates is probably associated with the increased difficulty in determining the smallest relaxation rate, because of a smaller signal-to-noise ratio at this frequency.

The relaxation rate determined by extrapolating to $\tau^2 = 0$ in Figs. 6 and 7 gives a value of $T_1 = 950$ μsec for the nonspectral-diffusion relaxation processes. This value is approximately 0.3 times the intrinsic Co^{59} single-domain longitudinal relaxation time of 3200 μsec.[23,24] This suggests that the spins observed in the rf skin depth by the stimulated-echo technique may be relaxed by fluctuating fields from neighboring unsaturated particles in a manner similar to the way spins are relaxed in the wings of Bloch walls.

B. Macroscopic Theory

Since $T_2 \ll T_1$, quasiequilibrium considerations are appropriate for describing the spectral-diffusion relaxation process. In a time of order T_2 after the spin system has been disturbed from its equilibrium state, local equilibrium is established in the subsystems of the spin packet. Then, the state of a subsystem is characterized by its Zeeman energy density function $\langle H(\omega)\rangle\rangle = -\hbar\omega\langle I^z(\omega)\rangle$, where ω refers to homogeneous frequencies, and the ensemble average is taken over the nonequilibrium density matrix. The spin temperature is well defined for each subsystem although the various spin temperatures have a slowly varying time dependency, quasiequilibrium. From quasithermodynamical theory, the deviation of the Zeeman energy density currents from their equilibrium value $\langle J(\omega)\rangle - \langle J(\omega)\rangle\rangle_L$ and the derivatives of the entropy $\partial S/\partial\langle H(\omega)\rangle\rangle$ can be represented by a linear expansion in the parameters $\langle H(\omega)\rangle - \langle H(\omega)\rangle_L$. Therefore, the mutual linear dependence of the quantities

$$\langle J(\omega)\rangle - \langle J(\omega)\rangle\rangle_L \quad \text{and} \quad \frac{\partial S}{\partial\langle H(\omega)\rangle\rangle}$$

may be written

$$\langle J(\omega)\rangle - \langle J(\omega)\rangle\rangle_L = \frac{1}{K\beta_L} \sum_{\omega'} L(\omega\omega') \frac{\partial S}{\partial\langle H(\omega')\rangle\rangle} . \tag{11}$$

Here $K\beta_L$ is the reciprocal-lattice temperature, K is the Boltzmann constant, and $L(\omega, \omega')$ are the kinetic coefficients. From thermodynamics and the spin temperature assumption, $\partial S/\partial\langle H(\omega')\rangle$ may be rewritten

$$\frac{\partial S}{\partial\langle H(\omega')\rangle} = \frac{K\partial\beta(\omega')}{\partial\omega'} \Delta\omega' ,$$

where $K\beta(\omega')$ is the reciprocal spin temperature of the spins of frequency ω'. In the case studied here, there is no macroscopic spectral current flow in the equilibrium state and $\langle J(\omega)\rangle_L$ is set equal to ze-

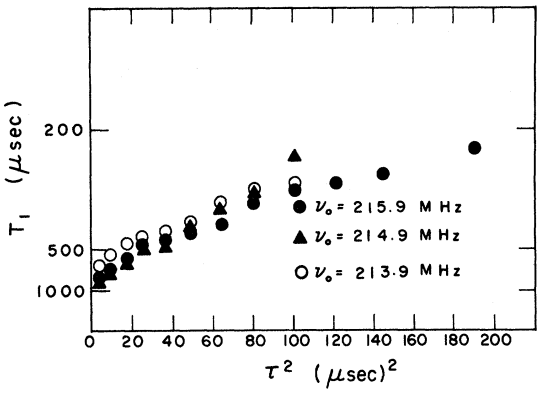

FIG. 7. Longitudinal relaxation rate versus τ^2 and frequency.

ro. $\langle J(\omega)\rangle$ satisfies the continuity equation

$$\frac{\partial}{\partial t}\langle H(\omega)\rangle = \frac{-\partial}{\partial \omega}\langle J(\omega)\rangle .$$

Thus, a general spectral-diffusion equation is written in the limit of a continuous frequency distribution:

$$\frac{\partial}{\partial t}\langle H(\omega)\rangle = -\frac{\partial}{\partial \omega}\int_{-\infty}^{\infty} L(\omega,\omega')\frac{1}{\beta_L}\frac{\partial \beta(\omega')}{\partial \omega'}\,d\omega' . \tag{12}$$

The theory of quantum statistics of irreversible processes gives the following prescription[9,10] for determining the kinetic coefficients:

$$L(\omega,\omega') = \lim_{s\to+0}\int_0^{\beta_L} d\lambda \int_{-\infty}^{0} e^{st}\langle J(\omega)J(\omega', t+i\hbar\lambda)\rangle_L\, dt$$

$$\cong \lim_{s\to+0}\beta_L\int_{-\infty}^{0} e^{st}\langle J(\omega)J(\omega',t)\rangle_L\, dt . \tag{13}$$

The current operator is determined from the equation of motion of $H(\omega)$ and the continuity equation. Consider,

$$\frac{\partial J(\omega)}{\partial \omega} = -\frac{\partial H(\omega)}{\partial t} = -\sum_{I\in\omega}\frac{\partial H_I^z}{\partial t}$$

$$= -i\omega\sum_{I\in\omega}\sum_{j\neq I} A_{Ij}(I_I^+ I_j^- - I_I^- I_j^+) ,$$

then

$$J(\omega) = -i\int_{-\infty}^{\omega}\omega'\sum_{I\in\omega}\sum_{j\neq I} A_{Ij}(I_I^+ I_j - I_I^- I_j^+)\,d\omega', \tag{14}$$

$$J(-\infty) = 0 .$$

When the current operator is substituted into Eq. (13) and the high-temperature approximation is made, the correlation function is given by the results of the microscopic theory in Sec. IIB. The integral over time is essentially the Fourier transform of the square of the relaxation function, and the various frequency integrals are simplified because of the criterion that no correlation exists between spins at different sites, placing a δ-function criterion on the intermediate frequencies.[16] The only serious approximation that is necessary to evaluate $L(\omega,\omega')$ is the assumption that the relaxation function is purely exponential. It will be shown later that this has serious consequences in limiting the description of the spectral-diffusion process. However, with the choice of the frequency cutoff made in Sec. II, the long-time diffusion process is still described quantitatively. With this approximation in mind, $L(\omega,\omega')$ is substituted in Eq. (12) to give

$$\frac{\partial H(\omega)}{\partial t} = 2[\tfrac{2}{3}(I)(I+1)]^2\omega^2\sum_{I\in\omega}\sum_{j\neq i} A_{ij}^2$$

$$\times\left(\frac{T_2(\omega,\omega_j)}{1+(\omega-\omega_j)^2 T_2(\omega,\omega_j)}\right)[\beta(\omega)-\beta(\omega_j)] , \tag{15}$$

where

$$\frac{1}{T_2(\omega,\omega_j)} = \frac{1}{T_2(\omega)} + \frac{1}{T_2(\omega_j)} .$$

The spectral-diffusion process is driven by the difference in spin temperature across the spin packet which explains the τ dependence of the relaxation rate. At this point, it is again assumed that the microscopic inhomogeneity is spatially random and that frequency can be averaged over position. Substituting for $\sum_{I\in\omega} Ng(\omega-\omega_0)$, and using $g(\omega_j-\omega_0)$ to average frequency over the jth position, the summation over j can be made. The Lorentzian is more sharply peaked than $g(\omega_j-\omega_0)$ so that $g(\omega_j-\omega_0)$ will be set equal to $g(\omega-\omega_0)$ in the integral over ω_j. Also, for the same reason, $T_2(\omega,\omega_j)$ is set equal to $T_2(\omega,\omega) = \frac{1}{2}T_2(\omega)$. However, it is necessary to remember at this point that the assumption of exponential decay is only good for the Lorentzian linewidth limited to $|\omega-\omega_0| \leq \frac{1}{2}\omega_{SN}$. In order to relate the theory to the experimental results, the following relations:

$$\beta(\omega) = \cos(\omega-\omega_0)\tau\,\beta(\omega_0)$$

(coherent excitation is assumed which does not affect the final results),

$$\langle I^z(\omega)\rangle = \tfrac{1}{3}Ng(\omega)(I)(I+1)\hbar\omega\beta(\omega) ,$$

and finally from Sec. II

$$\frac{1}{T_2(\omega)} = \tfrac{4}{3}(I)(I+1)\sum_{j\neq i}\frac{A_{ij}^2}{\hbar^2}\pi g(\omega-\omega_0) ,$$

are used with the above considerations to give the final results

$$\frac{\partial}{\partial t}\langle I^z(\omega_0)\rangle = \frac{-1}{\pi}\left(\int_{\omega_0-\omega_{SN}/2}^{\omega_0+\omega_{SN}/2}\frac{1-\cos(\omega_j-\omega_0)\tau}{1+(\omega_j-\omega_0)^2[\frac{1}{2}T_2(\omega_0)]^2}\right)$$

$$\times\, d\omega_j\,\langle I^z(\omega_0)\rangle . \tag{16}$$

Thus, the spectral-diffusion decay is predicted to be exponential with a relaxation rate given by

$$\frac{1}{T_S} = \frac{1}{\pi}\left(\int_{\omega_0-\omega_{SN}/2}^{\omega_0+\omega_{SN}/2}\frac{1-\cos(\omega_j-\omega_0)\tau}{1+(\omega_j-\omega_0)^2[\frac{1}{2}T_2(\omega_0)]^2}\,d\omega_j\right). \tag{17}$$

To explain the disagreement between this result and the experimental results in Fig. 5, consider Eq. (17) in the random-walk limit $\tau \ll T_2$. In this limit,

$$1-\cos(\omega_j-\omega_0)\tau \cong \tfrac{1}{2}(\omega_j-\omega_0)^2\tau^2$$

and

$$1/T_S = D\tau^2 ,$$

where

$$D=\frac{2}{\pi}\frac{\{\omega_{SN}T_2(\omega_0)-4\tan^{-1}[\frac{1}{4}T_2(\omega_0)\omega_{SN}]\}}{T_2^3(\omega_0)} \quad . \qquad (18)$$

The spectral-diffusion relaxation rate is directly proportional to the cutoff in this limit. This result shows the limitation of the simple cutoff model. In actuality, the line is Gaussian in the wings, which would thus lead to a distribution of relaxation rates. However, in the derivation, the functional form of the relaxation function was too complex to handle in closed form. Even so, the choice of cutoff should give a lower limit for the diffusion constant, and thus, the simplified model should describe the long-time spectral diffusion process.

In Fig. 6, the numerical integration of Eq. (17) is represented by the full line. The theoretical curve was adjusted to fit at $\tau^2=0$. It is seen that the agreement with data for all τ is quite good. For comparison, the dashed line gives the predicted spectral-diffusion relaxation rate for a Gaussian relaxation function $\phi(t)=e^{-t^2/2T_2^2}$. For this relaxation function,

$$1/T_s(\text{Gaussian})=2/T_2(1-e^{-\tau^2/T_2^2}),$$

which is to be compared with Eq. (17) which gives

$$1/T_S=2/T_2(1-e^{-2\tau/T_2})$$

in the limit $\frac{1}{2}\tau\omega_{SN}\to\infty$. Both functions lead to a maximum relaxation rate of $2/T_2$; however, the Gaussian relaxation function leads to saturation much more rapidly than do the observed experimental results. Also Eq. (18) predicts a diffusion constant $D\cong 0.5/T_2^3$ in qualitative agreement with the observed value $0.85/T_2^3$ while $1/T_2$(Gaussian) gives $D=2/T_2^3$ which is close to the value observed for the short-time diffusion process. Using Eq. (18) and the values of T_2 determined in Fig. 3, D is calculated to decrease only 6% in going from 215.9 to 213.9 MHz. The increase in the numerator and denominator essentially compensate for each other in agreement with the results of Fig. 7. Considering the uncertainty in choosing the cutoff, and the obvious oversimplification of the actual experimental situation, this agreement between theory and experiment is quite remarkable. The simple model of the homogeneous line, Lorentzian of width T_2^{-1} and the cutoff $\frac{1}{2}\omega_{SN}$ gives a simple physical picture of the spectral-diffusion problem.

IV. APPARATUS

The main considerations in designing and building the transient study apparatus[16] were detection sensitivity and minimizing the adverse effect the large rf pulses have on the detection system (see block diagram in Fig. 8). A random-phase pulsed oscillator of the Arenberg PG 650 design, which delivered approximately 20 W of peak power at 200 MHz when inductively coupled to the series-tuned sample network, was used to resonate the Co^{59} sample. The nuclear-induction signal was detected by a wide-band converter which consisted of a two-stage grounded-grid preamplifier and a pentode mixer and cathode-follower stage. The low Q value of 10–15 for the preamplifier stages and the mixer stages prevented excessive ringing following the large rf pulses. The converter was linear over the 30-dB signal range studied and had a measured sensitivity greater than 3 μV. The i.f. amplifier was most vulnerable to saturation, and since it was preceded by an attenuator, saturation was more of a problem at small signals. Diode gates were placed after the local oscillator and after the converter and were closed during the pulse excitation in order to minimize saturation in the i.f. amplifier. Although diode gates have limited effectiveness in the 30–200-MHz frequency range, measurements could be made as close as 1 μsec after an rf pulse at large signals. A precision attenuator was used to maintain a constant nuclear induction signal at the i.f. detector input, so that the measurements were independent of the detector response. Since the smallest increment of attenuation was 1 dB, it was necessary to extrapolate for signal changes less than this amount.

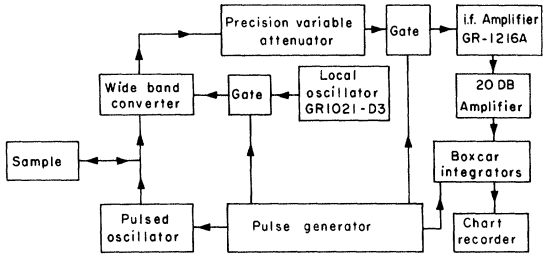

FIG. 8. Block diagram of the apparatus.

ACKNOWLEDGMENTS

I thank Dr. A. M. Portis for suggesting this problem. Dr. Portis's physical insights made the experimental execution and theoretical interpretation possible. I thank Dr. E. L. Hahn for an enlightening discussion of the oscillatory effect. The computer program was very kindly written by Richard Johnson. I thank Dr. J. N. Aubrun for his help in building some of the apparatus. This work was supported by the U.S. Atomic Energy Commission.

*Present address: Bell Telephone Laboratories, Murray Hill, N. J.

[1]A. C. Gossard and A. M. Portis, Phys. Rev. Letters 3, 164 (1959); A. M. Portis and A. C. Gossard, J. Appl. Phys. Suppl. 31, 205 (1960).

[2]H. Suhl, Phys. Rev. 109, 606 (1958); T. Nakamura, Prog. Theoret. Phys. (Kyoto) 20, 542 (1958).

[3]E. D. Shaw, Bull. Am. Phys. Soc. 14, 540 (1969).

[4]E. L. Hahn and D. E. Maxwell, Phys. Rev. 88, 1070 (1952).

[5]R. Kubo and K. Tomita, in *Proceedings of the International Conference on Theoretical Physics, Kyoto and Tokyo, September* 1953 (Science Council of Japan, Tokyo, 1954), p. 779.

[6]A. M. Portis, Phys. Rev. 104, 584 (1956).

[7]P. Pincus, V. Jaccarino, D. Hone, and T. Ngwe, Phys. Letters 27, 54 (1968); D. Hone, V. Jaccarino, T. Ngwe, and P. Pincus, Phys. Rev. 186, 291 (1969).

[8]G. E. Pake, *Paramagnetic Resonance* (Benjamin, New York, 1962), p. 91.

[9]R. Kubo, in *Lectures in Theoretical Physics*, edited by Wesley E. Britton and Lita G. Dunham (Interscience, New York, 1959), Vol. 1, p. 120.

[10]D. N. Zubarev, Dokl. Akad. Nauk SSR 140, 92 (1961) [Soviet Phys. Doklady 6, 776 (1962)].

[11]L. L. Buishvili and D. N. Zubarev, Fiz. Tverd. Tela 7, 722 (1965) [Soviet Phys. Solid State 7, 580 (1965)].

[12]M. Weger, A. M. Portis, and E. L. Hahn, J. Appl. Phys. 32, 124S (1961); M. Weger, thesis, University of California, 1960 (unpublished).

[13]E. L. Hahn, Phys. Rev. 80, 580 (1950).

[14]J. Barak and N. Kaplan, Phys. Rev. Letters 23, 925 (1969). I am grateful to Professor V. Jaccarino for calling my attention to this work.

[15]A. C. Gossard, A. M. Portis, M. Rubinstein, and R. H. Lindquist, Phys. Rev. 138, A1415 (1965).

[16]E. D. Shaw, thesis, University of California, 1969 (unpublished).

[17]F. Keffer, in *Handbuch der Physik*, edited by S. Flügge (Springer, Berlin, 1966), Vol. 18, p. 258.

[18]Reference 17, p. 227.

[19]This result was reported in private correspondence to E. L. Hahn for spin-$\frac{1}{2}$ particles.

[20]G. E. Pake, *Paramagnetic Resonance* (Benjamin, New York, 1962), p. 135.

[21]J. R. Klauder and P. W. Anderson, Phys. Rev. 125, 912 (1962).

[22]A. M. Portis, Phys. Rev. 91, 1070 (1953).

[23]R. E. Walstead, V. Jaccarino, and N. Kaplan, Phys. Letters 23, 514 (1966).

[24]N. Kaplan, V. Jaccarino, and R. T. Lewis, J. Appl. Phys. 39, 500 (1968).

PHYSICAL REVIEW B VOLUME 2, NUMBER 7 1 OCTOBER 1970

Temperature-Dependent Optical Mode in Antiferroelectric $PbZrO_3$ by the Mössbauer Effect

A. P. Jain, S. N. Shringi,* and M. L. Sharma
National Physical Laboratory, New Delhi, 12 India

(Received 8 April 1970)

The Mössbauer effect for Sn^{119m} in the $PbZrO_3$ lattice has been studied from 27 to 320 °C, with particular emphasis on the region near the Curie temperature. The Mössbauer fraction changes by $(40 \pm 8)\%$ at the transition temperature T_C from its value at room temperature. This is to be compared with the corresponding change of 10% for the earlier ferroelectric $BaTiO_3 : Sn^{119m}$ system. These results are consistent with Dvorak's suggestion that in antiferroelectrics the frequency over the entire optical branch may vanish at T_C. A sharp change in the isomer shift and the vanishing of the electric field gradient has also been observed, as is expected from the change in the crystal structure at T_C.

I. INTRODUCTION

Ferroelectricity in perovskite-type crystals such as $BaTiO_3$ and $SrTiO_3$ has lately been a subject of considerable experimental investigations by means of various techniques: the Mössbauer effect,[1] neutron scattering,[2] and dielectric-constant measurements.[3] The main reason for this increased activity has been the theory of Cochran, who describes ferroelectricity in these crystals as being due to the occurrence of instabilities in the lattice-dynamical modes (particularly the optical modes) at the ferro-to-para transition temperature.[4] In fact, it has been suggested that $\omega_T^2 \propto (T - T_c)$, where ω_T is the frequency of the transverse optical mode at $K = 0$, and T_C is the transition temperature. Such a behavior of $(\omega_T^2)_{K=0}$ near the transition temperature has been verified in $SrTiO_3$ by studies of neutron scattering,[2] and in Co^{57}-doped $BaTiO_3$ by the Mössbauer effect.[1]

It has recently been suggested that in antiferroelectrics the entire optical branch may be temperature dependent near the transition temperature, in contrast with ferroelectrics, where only